*Int. J. Chem. Technol.***2025,** 9(1)**,** 41-49.
DOI: http://dx.doi.org/10.32571/ijct.1561919

Serradj and co-workers
E-ISSN: 2602-277X

International Journal of Chemistry and Technology

http://dergipark.org.tr/ijct

Research Article

Structured Cupric Oxide Grown on Copper Sheet as an Effective Electrocatalyst Towards Hydrogen Peroxide Reduction Reaction

Abdennour SERRADJ[1, 2], Charif DEHCHAR*[2, 3], Djamel SELLOUM[2, 3], Ahmed ZOUAOUI[2]

[1] *Department of Process Engineering, Faculty of Technology, University Kasdi Merbah, 30000, Ouargla, Algeria*

[2] *Laboratoire Croissance et Caractérisation de Nouveaux Semi-conducteurs, Université Ferhat Abbas, Sétif-1, 19000, Sétif, Algérie.*

[3] *Department of Chemistry, Faculty of Sciences, University of Ferhat Abbas Setif 1, 19137 Setif, Algeria.*

Received: 5 October 2024; Revised: 6 January 2025; Accepted: 16 January 2024

*Corresponding author: dcharif@hotmail.fr

Citation: Serradj, A., Dehchar, C., Selloum, D., Zouaouı, A. *Int. J. Chem. Technol.* **2025**, 9(1), 41-49.

ABSTRACT

In this work, a highly efficient and cost-effective electrode material based on a cupric oxide (CuO) thin film was synthesized, and its electrocatalytic activity towards the reduction of hydrogen peroxide (H_2O_2) was investigated. The CuO film was formed on a copper (Cu) sheet using a direct electrochemical oxidation method in an alkaline medium (4–6 M KOH). This approach enabled the superficial oxidation of the Cu sheet, resulting in the formation of an oxidized layer on its surface. X-ray diffraction (XRD) analysis confirmed the formation of a high-purity CuO film with remarkable crystallinity. Scanning electron microscopy (SEM) revealed that the film possesses a highly rough surface and a homogeneous microstructure. The electrocatalytic performance of the CuO/Cu electrode for the H_2O_2 reduction reaction was studied in 0.1 M KOH electrolyte using cyclic voltammetry and chronoamperometry techniques. Optimization of the synthesis process showed that the concentration of the KOH electrolyte is critical for the growth of the CuO film and the activity of the catalyst. The effects of H_2O_2 concentration and potential scan rate on the electrode response were also examined. Under optimized conditions, the CuO/Cu catalyst exhibited excellent performance, displaying an extremely high cathodic overpotential of –0.4 V at a broad reduction current density. Additionally, the electrode demonstrated significant electrochemical stability after prolonged reduction testing. These results suggest that the CuO/Cu electrode has the potential to be an effective cathode electrocatalyst for applications in fuel cells utilizing H_2O_2 as an oxidant.

Keywords: Cupric oxide, electrocatalyst, fuel cell, hydrogen peroxide.

1. INTRODUCTION

Global energy issues and increasing concerns about climate change have intensified research and development of clean and sustainable energy technologies. Fuel cells have gained attention as a highly efficient and eco-friendly technology for energy conversion, suitable for a range of applications, including portable, mobile, and stationary systems.[1,2] By operating through electrochemical reactions that generate electricity, fuel cells offer an attractive alternative to fossil fuels, providing a wide variety of environmental benefits.[3,4] However, despite their potential, fuel cells are not yet sufficiently mature for large-scale commercialization. Several technological and economic challenges hinder their widespread adoption.[5] One of the primary challenges is the high cost of catalyst materials like platinum and ruthenium, which continues to pose a significant barrier.[6,7] Additionally, limitations related to the membranes used in fuel cells add further complexities, increasing manufacturing costs and reducing the overall efficiency of energy conversion.[8,9]

These challenges underscore the urgent need for the development of cost-effective catalysts and the enhancement of membrane performance, or alternatively, the reconsideration of fuel cell designs that eliminate the need for membranes. Several research groups have explored the use of platinum group metal-free electrocatalysts, including carbon-based materials, transition metals and their oxides.[10] Additionally, alternative fuels such as borohydride[11], methanol[12], ethanol[13], glucose[14-16], ethylene glycol[17], and ammonia[18], which offer the potential for higher open-circuit voltages and current densities compared to hydrogen/oxygen fuel cells, have been proposed. Some of these fuels, such as ethanol, can be derived from biomass.[19]

Besides, there is considerable interest in exploring hydrogen peroxide (H_2O_2) as an alternative to oxygen for fuel cells. As an oxidant, H_2O_2 may enhance performance, prevent water flooding due to its liquid phase, and ensure air independence, thereby expanding applications to oxygen-free environments such as space and underwater. Moreover, the electroreduction of H_2O_2 is feasible in both acidic and alkaline media, making it suitable for use in acidic, alkaline, and hybrid-type fuel cells. Recently, various fuels have been investigated for their compatibility with H_2O_2, including borohydride[20,21], ethanol[22], hydrazine[23,24], and formic acid.[25]

Additionally, serving dual roles as an oxidant and a fuel, H_2O_2 presents opportunities for simplified fuel cell designs and cost reduction.[26-29] However, despite its promising potential as an alternative fuel, its practical application in electrochemical systems faces challenges, including limited stability over time and handling difficulties due to its strong oxidizing nature, which must be addressed to unlock its full potential.[30-32]

The current study focuses on developing a new electrode material based on copper oxide (CuO) film formed on a copper (Cu) sheet through a facile electrochemical oxidation process for the electroreduction of H_2O_2 in an alkaline medium. The choice of CuO is driven by its advantageous properties, including ease of synthesis, relatively low cost, and both chemical and electrochemical stability. The primary objective is to develop an electrode that can efficiently catalyze the H_2O_2 reduction reaction while also being easy to prepare and economically viable for large-scale applications.

This study encompasses the preparation, physicochemical characterization, and evaluation of the electrocatalytic activity of the CuO/Cu electrode for the electroreduction of H_2O_2. A comprehensive analysis of potential electrochemical reactions is presented, and factors influencing the electrocatalytic performance of the CuO/Cu electrode are discussed.

2. EXPERIMENTAL

2.1. Materials and Reagents

The preparation of the CuO film was achieved through direct alkaline electrochemical oxidation of metallic copper (Cu) plates measuring 2×1 cm^2, cut from a copper sheet with a thickness of 1 mm (ASTM C10200, Cu 99.9%, resistivity at 20 °C = 1.72 μΩ.cm) purchased from LAYMORE. This substrate was chosen mainly for its high purity, outstanding electrical conductivity, and resistance to corrosion.

The electrolyte used for the preparation of CuO film is an aqueous solution of potassium hydroxide (KOH, Prolabo, 99%). Different concentrations of this electrolyte (from 4 to 6 M) were tested to optimize the best preparation conditions. Diluted KOH solutions may not yield films with comparable quality in which copper surface remains almost unchanged.[33]

Before the electrochemical deposition of the CuO film, the Cu plate was sonicated in acetone (VWR, 99%) for 5 minutes and washed with distilled water. Following this, it was etched in a 2 M hydrochloric acid (HCl, VWR, 37%) solution for 10 minutes and again washed with distilled water. The treated Cu plate was then electrochemically oxidized in a KOH solution. Finally, the sample was rinsed thoroughly with distilled water and left to air dry.

2.2. Equipments and Methods

Cyclic voltammetry was used to prepare the CuO/Cu electrode in KOH solution by sweeping the potential from –0.45 to 0.0 V with a scan rate of 10 mV s^{-1}. The electrocatalytic activity of the prepared CuO/Cu catalyst for the reduction of hydrogen peroxide (H_2O_2, VWR, 30%) was studied in 0.1 M KOH aqueous solution using cyclic voltammetry and chronoamperometry.

Electrochemical measurements were conducted at room temperature (22 ± 2 °C) using a Biologic SP-300 potentiostat and a conventional three-electrode cell. The working electrode was either a Cu plate or CuO/Cu with a surface area of 1 cm^2, while the counter electrode was a platinum (Pt) foil (1 cm^2), and the reference electrode was a saturated calomel electrode (SCE).

The morphological characterization of the CuO film was conducted using a JEOL NeoScope Scanning Electron Microscope (SEM), while the crystallinity was analyzed with an X'pert PROMPD PANalytical diffractometer utilizing Cu Kα radiation ($\lambda = 1.5406$ Å) over a 2θ range of 25–90°. Fourier Transform Infrared (FT-IR) analysis, with an IRSpirit FTIR spectrophotometer (Shimadzu), was carried out to show the presence of chemical bonds of Cu–O.

DOI: http://dx.doi.org/10.32571/ijct.1561919 **E-ISSN: 2602-277X**

3. RESULTS and DISCUSSION

3.1. Preparation of CuO Film

The formation of the CuO film on the copper substrate (Cu 10200) was carried out by electrochemical oxidation via cyclic voltammetry in an aqueous KOH solution (pH = 12.5–13). As a first step, a KOH concentration of 5 M was used. Subsequently, this concentration was optimized by testing the preparation with different concentrations. The obtained voltammogram is presented in Figure 1a. The potential was varied between –0.45 and 0.0 V vs. SCE with a sweep rate of 10 mV s^{-1}.

On this voltammogram, it can be noted that during the potential scan in the anodic direction, a pronounced anodic peak appears centered at –0.22 V vs. SCE. This peak is attributed to the oxidation of the copper plate, leading to the formation of a black film characteristic of the cupric oxide, CuO, according to the following equation:

$$Cu_{(s)} + 2OH^{-}_{(aq)} \rightarrow CuO_{(s)} + H_2O_{(l)} + 2e^{-} \quad (1)$$

The decrease in oxidation current density observed at more anodic potentials (> –0.22 V vs. SCE) is attributable to the diffusion phenomenon, which limits the copper oxidation process.

The voltammogram indicates that copper oxidation in an alkaline medium is a very rapid reaction, generating approximately 45 mA cm^{-2} of current density for an overpotential of 0.1 V. The onset potential, marking the beginning of copper electrooxidation, is around –0.35 V vs. SCE. During the reverse potential scan in the cathodic direction, the current density remains constant and zero, confirming that a passivating film has formed on the electrode surface. This new phase is very stable in alkaline medium and does not easily reduce, which is consistent with the stability of CuO under alkaline pH conditions.[34]

To optimize the concentration of the electrolyte used in the growth of the CuO film, three different concentrations of KOH were examined: 4, 5, and 6 M. Figure 1b shows that all three cyclic voltammetry curves have a similar profile, displaying an anodic peak during the forward scan and a passivation plateau during the reverse scan.

The curves also show that the current density of the oxidation peak varies depending on the KOH concentration. The highest oxidation current density was observed at a concentration of 6 M. This concentration was chosen to prepare the electrode for further study. As we shall observe later, the CuO film obtained at this concentration demonstrated superior electrocatalytic activity for the reduction of hydrogen peroxide compared to the other concentrations.

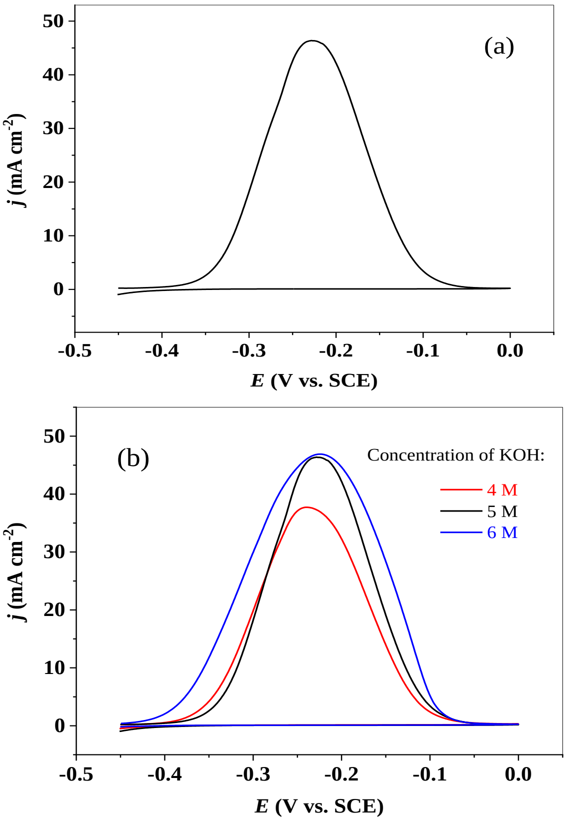

Figure 1. Cyclic voltammetry curves recorded on Cu plate: **(a)** in 5 M KOH electrolyte, and **(b)** at different concentrations of KOH (4, 5 and 6 M). Scan rate = 10 mV s^{-1}.

3.2. Characterization of CuO film

Figure 2a and b show SEM micrographs of the copper sheet (Cu 10200) before and after the formation of the CuO film, respectively. A comparison between these two images reveals a clear difference after the formation of the CuO film. Before oxidation, the copper substrate exhibits a smooth surface, whereas the oxidized sample is completely coated with a uniform and dense layer characterized by a lawn-like microstructure.

The high-magnification micrographs of the oxidized copper substrate (Figure 2c and d) indicate that the resulting CuO film is composed of a collection of numerous needle-shaped copper oxide crystals, which are randomly distributed across the entire surface of the copper substrate. According to the 43ort he43re, this type of oxide growth makes the electrode surface very accessible to reactants, thereby increasing the reactivity of the electrode.[35,36]

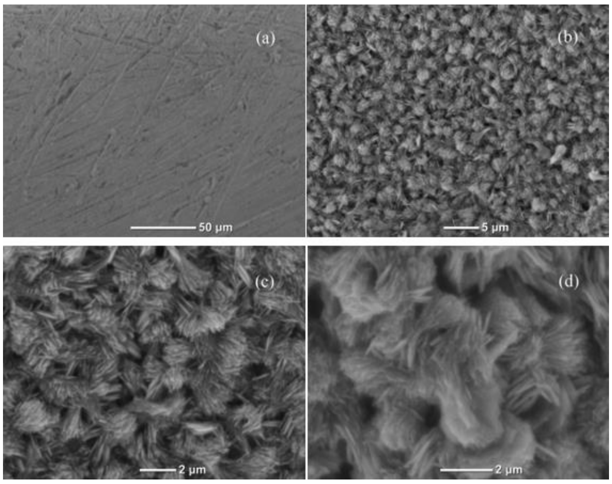

Figure 2. SEM micrographs of the Cu plate: **(a)** before and **(b)** after copper oxide layer formation; **(c)** and **(d)** are enlargements of image **(b)**.

Figure 3 displays the X-ray diffraction spectra 44ort he copper substrate before and after electrochemical oxidation. The diffraction peaks for both samples appear at 2*θ* values of 43.42°, 50.53°, and 74.65° correspond to the (111), (200), and (220) diffraction planes of the face-centered cubic (fcc) structure of copper, respectively. The XRD spectrum of the oxidized copper sample reveals two additional diffraction peaks at 2*θ* = 33.8° and 37.9°, which can be attributed to the (002)-(111) and (200)-(111) planes of the monoclinic phase of CuO, respectively.[37,38]

Thus, one can conclude that the deposit formed consists of the monoclinic phase CuO. Moreover, the lack of impurity peaks and the sharpness of the peaks indicate that the formed CuO film is of high purity and high crystallinity.[39]

The mean size of the crystallites, calculated using Scherrer formula 44ort he (200) peak with the highest intensity, is 23.45 nm.

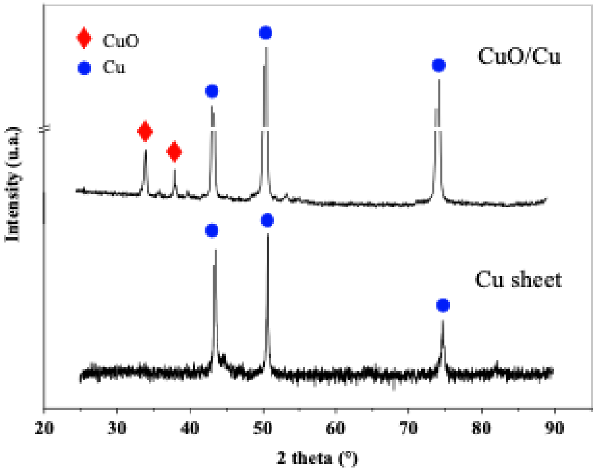

Figure 3. XRD patterns of Cu sheet before and after electrochemical oxidation in KOH electrolyte.

FT-IR spectroscopy is a useful technique for analyzing the presence of functional groups on the surface of samples. Figure 4 shows the FT-IR spectrum recorded in the range of 400–4000 cm^{-1} for the prepared CuO sample.

The observed peaks at 448, 510, 632, 681, and 919 cm^{-1} correspond to Cu–O stretching vibrations of monoclinic CuO.[40-42] This result further supports the formation of CuO.

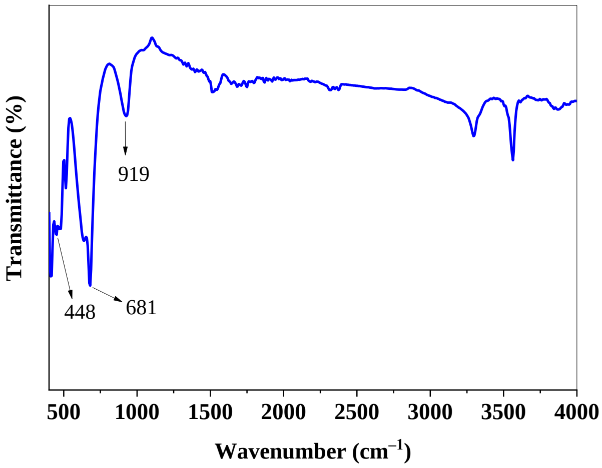

Figure 4. FT-IR spectra of the CuO/Cu sample.

3.3. Electroreduction of hydrogen peroxide

This section presents the results of the study regarding the electrocatalytic performance of the CuO/Cu electrode for the electroreduction of hydrogen peroxide in alkaline medium.

3.3.1. Response of CuO/Cu towards H_2O_2

The voltammograms shown in Figure 5 illustrate the response of the CuO/Cu electrode in the absence and presence of hydrogen peroxide (H_2O_2, 1 M) in 0.1 M KOH electrolyte. Measurements were conducted from –0.25 to –0.6 V vs. SCE, with a scan rate of 50 mV s^{-1}.

In the absence of H_2O_2, no anodic or cathodic peaks were observed within the applied potential range, indicating that no oxidation or reduction reactions occur at these potentials. However, when H_2O_2 was added to the KOH electrolyte, a significant increase in cathodic current was observed during the forward scan, appearing as a broad peak centered on –0.4 V vs. SCE. This peak corresponds to the reduction of H_2O_2 on the surface of the CuO/Cu electrode.

From this curve, it is also noteworthy that the electroreduction peak of H_2O_2, with an onset potential around –0.3 V vs. SCE, requires only an overpotential of approximately 0.1 V to reach its maximum current density (j_{max} = –0.33 mA cm^{-2}). This demonstrates a very rapid electroreduction kinetic, indicating significant electrocatalytic activity. This behavior is particularly promising for applications in electrochemical energy conversion, such as fuel cells using H_2O_2 as an oxidant.[43]

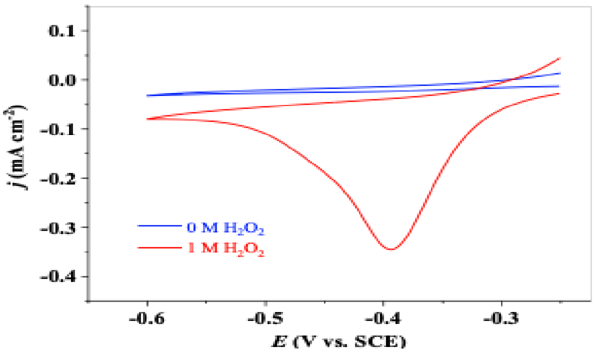

Figure 5. Cyclic voltammograms recorded on the CuO/Cu electrode (prepared from 6 M KOH) in the absence and presence of H_2O_2 (1 M) in 0.1 M KOH. Scan rate = 50 mV s^{-1}.

It is well established in the literature[44] that the electroreduction of H_2O_2 mainly occurs through two parallel processes: a direct pathway (without oxygen) and an indirect pathway (involving oxygen formation followed by its reduction) (Scheme 1).

The direct pathway is favored for several reasons: (1) the direct reduction of H_2O_2 is a two-electron process, which exhibits easier kinetics compared to oxygen reduction, a four-electron process; (2) the theoretical potential 45ort he direct reduction of H_2O_2 is greater than that for oxygen reduction, resulting in a higher cell voltage for the direct reduction of H_2O_2; (3) the indirect pathway requires gas management, which complicates system simplicity in fuel cells that utilize H_2O_2 as an oxidant. Therefore, to improve the performance of these fuel cells, cathode catalysts that selectively catalyze the electrochemical reduction of H_2O_2 via the direct pathway are necessary.

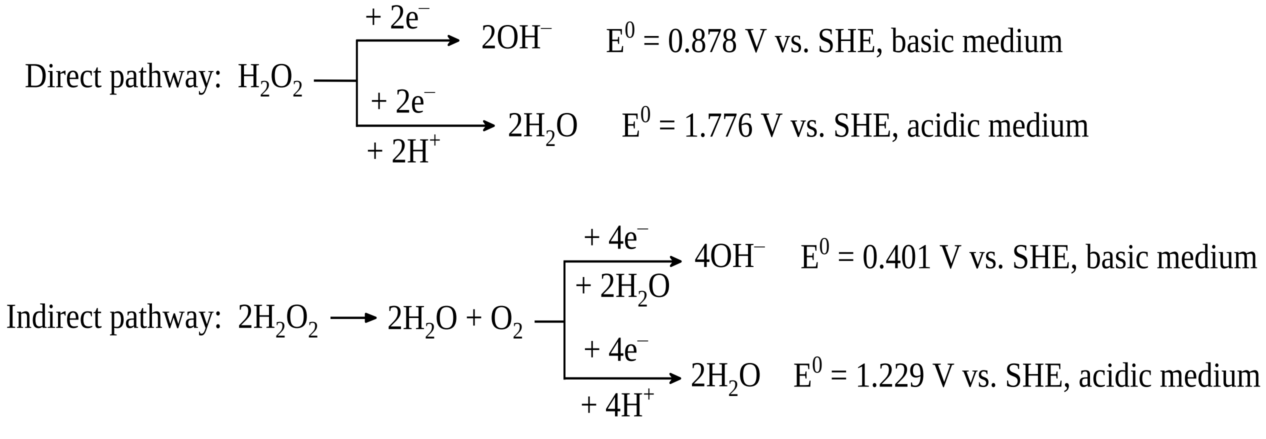

Scheme 1. The direct and indirect pathway for H_2O_2 electroreduction.

3.2. Effect of CuO film growth conditions

Figure 6 compares the responses of three CuO/Cu electrode materials for the reduction of hydrogen peroxide (H_2O_2, 1 M) in a 0.1 M KOH electrolyte. The electrodes were prepared by cyclic voltammetry using different concentrations of KOH, namely 4, 5 and 6 M, as described previously. It is evident that the three electrodes exhibit similar electrocatalytic behavior towards the electroreduction of H_2O_2, although the current densities vary significantly. The electrode prepared with a 6 M KOH concentration showed the best performance in terms of maximum reduction current density. This superior performance may be attributed to the larger specific surface area of this electrode compared to the other two electrodes.

This result demonstrates that the KOH concentration used for electrode preparation is a crucial parameter, as it directly influences the electrocatalytic activity of the electrode in H_2O_2 reduction. The optimal KOH concentration for preparing the CuO/Cu electrode is 6 M.

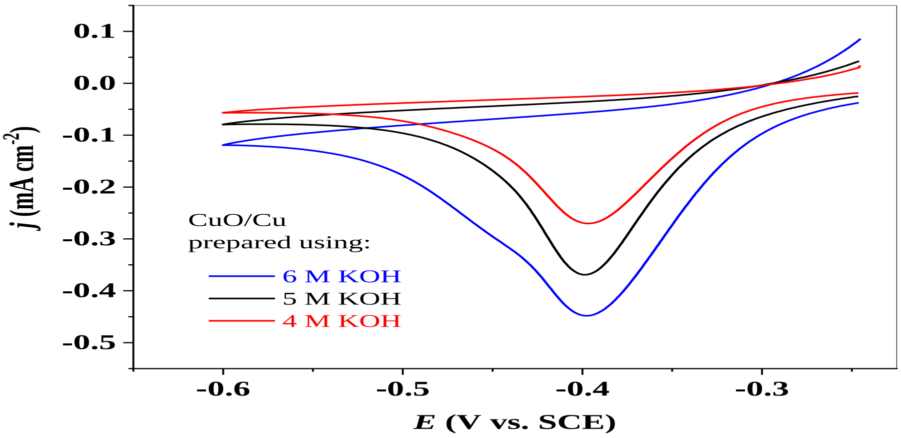

Figure 6. Cyclic voltammograms recorded on three CuO/Cu electrodes for which the CuO film was prepared from KOH solutions of different concentrations. Electrolyte: 0.1 M KOH + 1 M H_2O_2. Scan rate = 20 mV s^{-1}.

3.3.3. Effect of H_2O_2 Concentration

Figure 7 presents a series of CV curves recorded on the CuO/Cu electrode in 0.1 M KOH electrolyte containing different concentrations of H_2O_2, ranging from 0.25 to 1 M. It is evident that the reduction peak current density increases progressively with higher concentrations of H_2O_2 in the solution.

This result suggests that the CuO/Cu electrode exhibits electrocatalytic activity 46ort he reduction of H_2O_2. Moreover, the increase in current density indicates that this electrocatalytic activity was proportional to the amount of H_2O_2 present in the solution, and that the electrode can effectively catalyze the reduction of H_2O_2 even at varying concentrations, which is essential for applications in fuel cells.

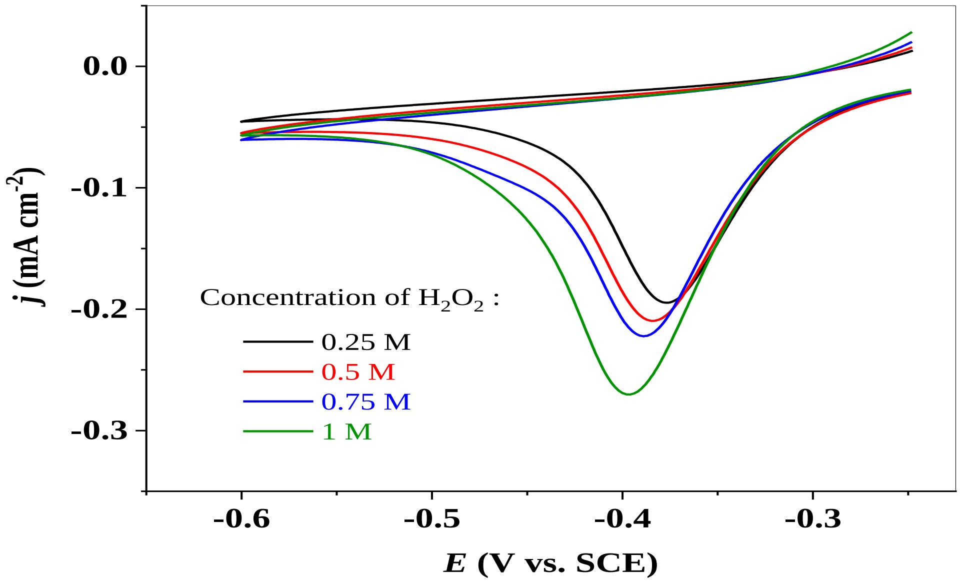

Figure 7. Cyclic voltammograms recorded on the CuO/Cu electrode in 0.1 M KOH in the presence of different concentrations of hydrogen peroxide. Scan rate = 20 mV s^{-1}.

3.3.4. Effect of scan rate

The influence of the potential scan rate was studied to highlight the factors limiting the electroreduction reaction of H_2O_2 on the CuO/Cu electrode surface. Figure 8a shows the CV curves recorded at different scan rates. The reduction peak current increased progressively with increasing scan rate. As shown in Figure 8b, a linear relatioship was observed between the reduction peak current and the scan rate within the range of 20 to 200 mV s^{-1}, with a regression coefficient (R^2) of 0.9831 and a slope of 0.63. This suggests that the reduction of H_2O_2 on the surface of the CuO/Cu electrode may be limited by the adsorption and diffusion of the reactants (H_2O_2) and products (OH^-).

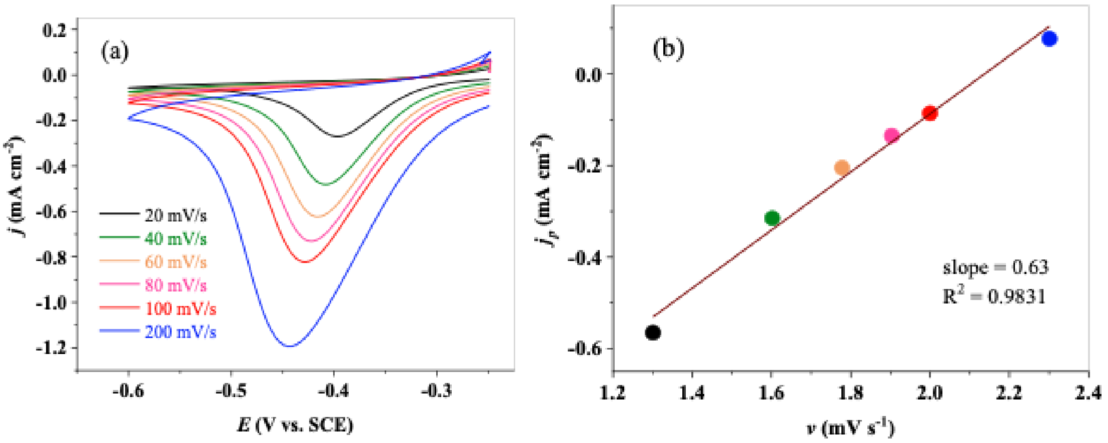

Figure 8.(a) Cyclic voltammograms recorded on the CuO/Cu electrode at scan rates of 20, 40, 60, 80, 100, and 200 mV s^{-1}. Electrolyte: 0.1 M KOH + 1 M H_2O_2. **(b)** Plot of peak current density against applied scan rates (log-log scale).

3.3.5. Stability test

The stability of the CuO/Cu electrode response was verified by examining the evolution of the H_2O_2 reduction current over time. This measurement was performed in potentiostatic mode for 2700 seconds, with the applied potential set to –0.3 and –0.4 V vs. SCE. The result obtained is presented in Figure 9. At an applied potential of –0.4 V vs. SCE, it is apparent that the reduction current density is relatively larger (j = –0.3 mA cm^{-2} against –0.18 mA cm^{-2} for the potential of –0.3 V vs. SCE). This difference in current density is in good agreement with the previously presented cyclic voltammetry results. Moreover, for both imposed potentials, a slight variation in the reduction current density can be observed over time. This result demonstrates acceptable stability for practical applications, confirming that the CuO/Cu electrode can maintain stable performance under prolonged operational conditions.

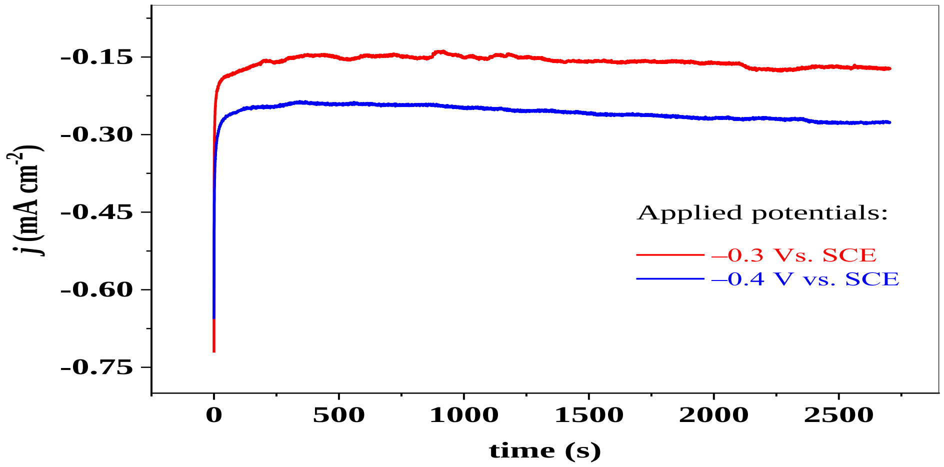

Figure 9. Current density-time curves showing the temporal evolution of the response of the CuO/Cu electrode in potentiostatic mode. Applied potentials = –0.3 and –0.4 V vs. SCE. Electrolyte: 0.1 M KOH + 1 M H_2O_2.

4. CONCLUSION

In summary, a microstructured CuO film was successfully synthesized via a facile electrochemical oxidation process in an alkaline medium on a copper sheet to fabricate a high-efficiency electrode for the hydrogen peroxide reduction reaction.

Scanning electron microscopy revealed a homogeneous microstructure, leading to enhanced electrocatalytic performance of the electrode. X-ray diffraction analysis confirmed the formation of a high-purity CuO film with remarkable crystallinity. The prepared electrodes showed excellent activity and notable stability for hydrogen peroxide reduction reaction in alkaline medium. The concentration of the KOH electrodeposition solution is a key parameter influencing the electrocatalytic activity of the electrode, with the best catalytic activity results obtained at a KOH concentration of 6 M.

The results obtained in this study open new perspectives for more efficient and sustainable fuel cells using hydrogen peroxide. Future work could involve testing the CuO catalyst under more realistic fuel cell operating conditions, such as in the presence of air and over extended cycling, to further evaluate its long-term stability and practical applicability.

Acknowledgements

This research is funded by the Ministry of Higher Education and Scientific Research of Algeria.

Conflict of Interest

The authors declare no competing interests related to the content of this article.

REFERENCES

1. An, L.; Zeng, L.; Zhao, T.S. Int. J. Hydrogen Energy **2013**, 38, 10602-10606.

2. Chu, S.; Majumdar, A. Nature **2012**, 488, 294-303.

3. Feiqi, L.; Fuquan, Z.; Zongwei, L.; Han, H. Int. J. Hydrogen Energy **2018**, 43, 22604-22621.

4. Qun, W.; Mianqiang, X.; Bin-Le, L.; Zhongfang, L.; Zhenya, Z. J. Clean. Prod. **2020**, 275, 123061.

5. Kampker, A.; Ayvaz, P.; Schön, C.; Karstedt, J.; Rörstmann, R.; Welker, F. Int. J. Hydrogen Energy **2020**, 45, 29288-29296.
6. Broizgou, A.; Song, S.Q.; Tsiakaras, P. Appl. Catal. B Environ. **2012**, 127, 371-388.

7. Wulandhari, S.; Sue, Y.T.; Wai, Y.W.; Fatin, S.O.; Ramya, K.; Shahid, M.; Arshid, N.; Rashmi, W.; Mohammad, K. J. Ind. Eng. Chem. **2023**, 122, 1-26.

8. Deuk, J.K.; Min, J.J.; Sang, Y.N. J. Ind. Eng. Chem. **2015**, 21, 36-52.

9. Peng, R.; Pucheng, P.; Yuehua, L.; Ziyao, W.; Dongfang, C.; Shangwei, H. Prog. Energy Combust. Sci. **2020**, 80, 100859.

10. Lo Vecchio, C.; Serov, A.; Dicome, M.; Zulevi, B.; Aricò, A.S.; Baglio, V. Electrochim. Acta **2021**, 394, 139108.

11. Lifeng, G.; Nie, L.; George, H.M. J. Power Sources **2007**, 173, 77-85.

12. Alias, M.S.; Kamarudin, S.K.; Zainoodin, A.M.; Masdar, M.S. Int. J. Hydrogen Energy **2020**, 45, 19620-19641.

13. Subrata, C.; Sweta, L.; Vinod, M.J.; Kirti, C.S.; Melepurath, D. J. Power Sources **2018**, 396, 725-733.

14. Debika, B.; Suddhasatwa, B. Electrochim. Acta **2010**, 55, 5775-5779.

15. Chikouche, I.; Dehchar, C.; Zouaoui, A.; Tingry, S.; Rezig, F.; Bouhcida, B. Surf. Rev. Lett. **2024**, 2450069-2450076.

16. Chikouche, I.; Dehchar, C.; Zouaoui, A.; Chia, A.; Cherora, Z. Surf. Rev. Lett. **2022**, 29, 2250143.

17. Zhefei, P.; Bin, H.; Liang, A. Int. J. Energy Res. **2018**, 1-9.

18. Wenzhi, L.; Yun, L.; Zhewei, Z.; Zhefei, P.; Rong, C.; Liang, A. J. Power Sources **2024**, 593, 233985.

19. Rajeswari, S.; Baskaran, D.; Saravanan, P.; Rajasimman, M.; Rajamohan, N.; Vasseghian, Y. Fuel **2022**, 317, 123448.

20. He, W.; Wang, L.; Yin, D.; Wang, S.; Liu, H.; Yu, W.; Sun, L.; Dong, X. Int. J. Hydrogen Energy **2024**, 71, 298-308.

21. Yin, X.; Zhu, K.; Ye, K.; Yan, J.; Cao, D.; Zhang, D.; Yao, J.; Wang, G. J. Power Sources **2022**, 541, 231704.

22. An, L.; Zhao, T.S. Int. J. Hydrogen Energy **2011**, 36,
9994-9999.

23. Hosseini, M. G.; Daneshvari-Esfahlan, V.; Aghajani, H.; Wolf, S.; Hacker, V. Catalysts **2021**, 11, 1372.

24. Yan, X.; Meng, F.; Xie, Y.; Liu, J.; Ding, Y. Sci. Rep. **2012**, 2, 941.

25. Déctor, A.; Esquivel, J.P.; González, M.J.; Guerra-Balcázar, M.; Ledesma-García, J.; Sabaté, N.; Arriaga, L.G. Electrochim. Acta **2013**, 92, 31-35.

26. Fukuzumi, S.; Yamada, Y.; Karlin, K.D. Electrochim. Acta **2012**, 82, 493-511.

27. Liang, A.; Tianshou, Z.; Xiaohui, Y.; Xuelong, Z.; Peng, T. Sci. Bull. **2015**, 60, 55-64.

28. Dehchar, C.; Chikouche, I.; Hamam, A.; Zouaoui, A.; Sahari, A.; Deflorian, F.; Belfar, S. Inorg. Chem. Commun. **2020**, 116, 107905.

29. Yamazaki, S.I.; Siroma, Z.; Senoh, H.; Ioroi, T.; Fujiwara, N.; Yasuda, K. J. Power Sources **2008**, 178, 20-25.

30. Zhou, X.; Zheng, X.; Li, M.; Fei, F.; Cao, X.; Dong, X.; Li, L.; Yuan, N.; Ding, J. Mater. Phys. Today **2024**, 44, 101432.

31. Wang, S.; Ye, D.; Liu, Z.; Zhu, X.; Chen, R.; Liao, Q.; Yang, Y.; Liu, H. Int. J. Hydrogen Energy **2022**, 47, 4793-4803.

32. Esan, O. C.; Shi, X.; Pan, Z.; Liu, Y.; Huo, X.; An, L.; Zhao, T. S. J. Power Sources **2022**, 548, 232114.

33. Fan, J.; Tang, D.; Wang, D. J. Alloys Compd. **2017**, 704, 624-630.

34. Zayyoun, N.; Bahmad, L.; Laânab, L.; Jaber, B. Appl. Phys. A **2016**, 122, 488.

35. Feng, Y.; Zheng, X. Nano Lett. **2010**, 10, 4762-4766.

36. Hamam, A.; Dehchar, C.; Maiza, M.; Chikouche, I.; Merabti, H. J. Electrochem. Sci. **2020**, 15, 3534-3542.

37. Cao, F.; Wang, T.; Ji, X. Appl. Surf. Sci. **2019**, 471, 417-424.

38. Ardekani, S.R.; Rouhaghdam, A.S.; Nazari, M. Chem. Phys. Lett. **2018**, 705, 19-22.

39. Xiao, B.; Wu, M.; Wang, Y.; Chen, R.; Liu, H. Chemistry Select **2020**, 5, 6075-6082.

40. Kumar, M. P.; Murugadoss, G.; Kumar, M. R. J. Mater. Sci.: Mater. Electron. **2020**, 31, 11286-11294.

41. Sukumar, S.; Rudrasenan, A.; Nambiar, D. P. ACS Omega **2020**, 5, 1040-1051.

42. Shinde, S. K.; Dubal, D. P.; Ghodake, G. S.; Gomez-Romero, P.; Kim, S.; Fulari, V. J. RSC Adv. **2015**, 5, 30478.

43. Miley, G.H.; Luo, N.; Mather, J.; Burton, R.; Hawkins, G.; Gu, L.; Byrd, E.; Gimlin, R.; Shrestha, P.J.; Benavides, G.; Laystrom, J.; Carroll, D. J. Power Sources **2007**, 165, 509-516.

44. Cao, D.; Sun, L.; Wang, G.; Lv, Y.; Zhang, M. J. Electroanal. Chem. **2008**, 621, 31-37